Headline Articles

p-tert-Butylthiacalix[6]arene as a Clustering Ligand. Syntheses and Structures of Co^{II}_5, Ni^{II}_4, and Mixed-Metal $M^{II}Ni^{II}_4$ (M = Mn, Co, and Cu) Cluster Complexes, and a Novel Metal-Induced Cluster Core Rearrangement

Takashi Kajiwara,* Reiko Shinagawa, Tasuku Ito,* Noriyoshi Kon,† Nobuhiko Iki,† and Sotaro Miyano*,†

Department of Chemistry, Graduate School of Science, Tohoku University, Aramaki, Aoba-ku, Sendai 980-8578

†Department of Biomolecular Engineering, Graduate School of Engineering, Tohoku University, Aramaki, Aoba-ku, Sendai 980-8579

Received June 4, 2003; E-mail: kajiwara@agnus.chem.tohoku.ac.jp

Using *p-tert*-butylthiacalix[6]arene (H_6L) as a clustering ligand, five cluster complexes having Co^{II}_5 (**2**), Ni^{II}_4 (**3**) and $M^{II}Ni^{II}_4$ (M = Co^{II} (**4**), Mn^{II} (**5**), and Cu^{II} (**6**)) cores were synthesized. In all the complexes except for **3**, a pinched conic L^{6-} acts as a pentanucleating ligand that involves a similar pyramidally arranged cluster core. Each mixed metal complex **4**–**6** involves four tetragonally arranged Ni^{II} ions occupying the basal plane of the pyramid and a M^{II} ion placed at the apex position. In **3**, H_2L^{4-} is in a cone conformation and the four Ni^{II} ions are arranged on the donor surface of H_2L^{4-} in a zigzag manner. The mixed metal complexes **4**–**6** are synthesized by reacting **3** and the appropriate $M(AcO)_2$ in a 1:1 ratio with a novel metal-induced core rearrangement occurring. In this reaction, the insertion of a M^{II} ion at the apex position forces the calixarene to take a cone conformation and the Ni^{II}_4 array rearranges to form a tetragonal cluster.

Multinuclear transition metal complexes have attracted much attention owing to the interesting properties and the functionalities. One approach to make multinuclear transition metal complexes is the use of multinucleating macrocyclic ligands.[1–12] Recent synthetic efforts along this line have been focused on making larger multinuclear complexes; in many cases, Schiff base ligands are used because they are easy to synthesize.[2–6] Thompson et al.[2a,b] and Robson et al.[2c] reported large macrocyclic ligands which can bind six metal ions inside the ligands. McKee and Shepard reported a flexible macrocyclic ligand which involves cubane-type tetramanganese(II) cluster core.[3] Many of the compounds synthesized in this way are homo-metal multinuclear complexes, although a few mixed metal multinuclear complexes have been also synthesized by step-by-step complexation.[4] For example, McKee et al. synthesized a mixed metal hexanuclear complex involving a cubane-type core which consists of a dinickel(II)dicopper(II) complex formed with a macrocyclic ligand and two external nickel(II) ions.[4a] Multinuclear complexes obtained by the use of Schiff base macrocyclic ligands are generally planar and hence any metal–metal interaction operates mainly in a two-dimensional manner.

In our studies aimed at the synthesis of large multinuclear or nano-sized metal complexes, we have been using a thiacalixarene and its derivatives as multinucleating ligands.[8,10–12] In the first report concerning *p-tert*-butylthiacalix[6]arene (H_6L), we showed the clustering ability of this ligand with the synthesis of a decacopper(II) complex, $[Cu_{10}(L)_2(\mu_3\text{-}O)_2(\mu_3\text{-}OH)_3(\mu\text{-}AcO)]$ (**1**).[12] In **1**, the hexaanionic L^{6-} acts as an undecadentate ligand via six phenoxo oxygens and five sulfurs, and a pentacopper(II) cluster core is included in the pocket formed by the L^{6-} which is in a pinched-cone conformation (Chart 1).

The five Cu^{II} ions are arranged in a square pyramidal manner, and the apex Cu^{II} ion is surrounded by a sulfur and four phenoxo oxygens (O2, O3, O5, and O6). The four basal Cu^{II} ions are located above these oxygen atoms and are additionally bridged by two phenoxo (O1 and O4), an oxo, an acetate, and a hydroxo group. The two pentacopper(II) units are connected via oxo and hydroxo groups to form decacopper(II) **1**. The calixarene supports the formation of a three-dimensional metal array in **1**, and ferromagnetic interactions among copper(II) ions arise from the orthogonality between the coordination planes of copper(II) ions. In this paper, we have extended our studies of $H_nL^{(6-n)-}$ with the synthesis of Co^{II}_5 (**2**), Ni^{II}_4 (**3**), and mixed-metal $Co^{II}Ni^{II}_4$ (**4**), $Mn^{II}Ni^{II}_4$ (**5**), and $Cu^{II}Ni^{II}_4$ (**6**) cluster complexes to further illustrate the ability of thiacalixarenes to form

Published on the web December 15, 2003; DOI 10.1246/bcsj.76.2267

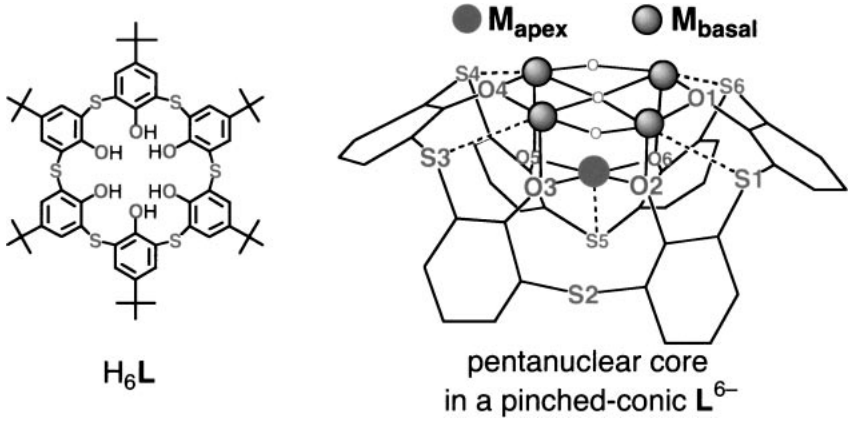

Chart 1.

large cluster complexes in a rational manner. The mixed-metal $M^{II}Ni^{II}_4$ cluster complexes are derived from the Ni^{II}_4 complex by a metal-induced Ni_4-core rearrangement reaction.

Experimental

Preparation. All solvents and chemicals were purchased as reagent grade and used without further purification. H_6L was prepared as described previously.[13]

[Co_5(L)(μ_4-OH)(μ-AcO)(μ-OMe)($MeOH)_4$]AcO (2). To a solution of H_6L (10.8 mg, 0.01 mmol) in CH_2Cl_2 (5 cm^3) was added a solution of $Co(OAc)_2 \cdot 4H_2O$ (24.9 mg, 0.10 mmol) in MeOH (5 cm^3) and the mixture was stirred at room temperature for 3 h. CH_3CN 1 cm^3 was added, and purple crystals precipitated (14.2 mg, 86%). The crystals were collected by filtration and dried in vacuo before elemental analysis was performed. Anal. Calcd for $[Co_5(C_{60}H_{66}O_6S_6)(\mu_4\text{-OH})(\mu\text{-}C_2H_3O_2)(\mu\text{-}CH_3O)(CH_3OH)_4]$-$(C_2H_3O_2)$: C, 49.91; H, 5.34%. Found: C, 49.91; H, 5.17%.

[$Ni_4(H_2L)(AcO)_4(\mu$-dmf)($dmf)_2$] (3). To a solution of H_6L (10.8 mg, 0.01 mmol) in $CHCl_3$ (2 cm^3) was added a solution of $Ni(OAc)_2 \cdot 4H_2O$ (24.9 mg, 0.10 mmol) in MeOH (1 cm^3) and the mixture was stirred at room temperature for 1 h. The solvent was removed by evaporation and the resultant powder was recrystallized from $CHCl_3$/DMF to give green crystals (11.9 mg, 67%). The crystals were collected by filtration and dried in vacuo. Anal. Calcd for $[Ni_4(C_{60}H_{68}O_6S_6)(\mu\text{-}C_2H_3O_2)_4(\mu\text{-}C_3H_7NO)$-$(C_3H_7NO)_2] \cdot CHCl_3 \cdot H_2O$: C, 49.17; H, 5.50; N, 2.21%. Found: C, 49.45; H, 5.47; N, 2.09%.

[$CoNi_4$(L)(μ_4-OH)(μ-AcO)$_2$(AcO)($H_2O)_2$($EtOH)$] (4). To a solution of **3** (17.7 mg, 0.01 mmol) in $CHCl_3$ (5 cm^3) was added a solution of $Co(OAc)_2 \cdot 4H_2O$ (2.49 mg, 0.01 mmol) in MeOH (1 cm^3) and the mixture was stirred at room temperature for 1 h. Addition of CH_3CN (2.5 cm^3) gave pale green crystals (15.0 mg, 91%). The crystals were collected by filtration and dried in vacuo. Anal. Calcd for $[CoNi_4(C_{60}H_{66}O_6S_6)(\mu_4\text{-OH})(\mu$-$C_2H_3O_2)_2(C_2H_3O_2)(H_2O)_2(C_2H_6O)] \cdot H_2O$: C, 49.10; H, 5.33%. Found: C, 49.00; H, 5.20%.

[$MnNi_4$(L)(μ_4-OH)(μ-AcO)$_2$(AcO)($H_2O)_2$($EtOH)$] (5). To a solution of **3** (17.7 mg, 0.01 mmol) in $CHCl_3$ (5 cm^3) was added a solution of $Mn(OAc)_2 \cdot 4H_2O$ (2.49 mg, 0.01 mmol) in MeOH (1 cm^3) and the mixture was stirred at room temperature for 1 h. The solution was evaporated to dryness and the resultant powder was recrystallized from $CHCl_3/CH_3CN$ to give pale green crystals (10.3 mg, 63%). Calcd for $[MnNi_4(C_{60}H_{66}O_6S_6)(\mu_4\text{-OH})(\mu$-$C_2H_3O_2)_2(C_2H_3O_2)(H_2O)_2(C_2H_6O)] \cdot H_2O$: C, 49.22; H, 5.34%. Found: C, 49.13; H, 5.33%.

[$CuNi_4$(L)(μ_4-OH)(μ-AcO)$_2$(AcO)($H_2O)_3$] (6). This complex was synthesized by a method similar to that for **5** using $Cu(AcO)_2$ and recrystallized from $CHCl_3$/DMF. Several crystals of **6** suitable for the X-ray crystallographic measurement were obtained. However, crystallization on a larger scale did not succeed, and therefore other physical measurements were not performed.

Structure Analyses. Measurements for all compounds were performed using a Bruker SMART CCD-based diffractometer with Mo Kα radiation ($\lambda = 0.71073$ Å). Because crystals of complexes **4** and **5** immediately lose solvent, the samples were sealed in glass capillaries with the mother liquor. Data collections for **4** and **5** were performed at room temperature, whereas measurements for other complexes were carried out at low temperature (180–223 K). The data integration and reduction were undertaken with SAINT and XPREP.[14] Absorption corrections were applied with SADABS supplied by G. Sheldrick (Universität Göttingen). The details of crystallographic measurements for all complexes are summarized in Table 1.

The structures were solved by direct methods with the SIR-92 program[15] and refined by least squares on F^2, SHELXL-97.[16] All non-hydrogen atoms were refined anisotropically. μ_4-OH^- hydrogen for **3** was found by D-Fourier technique and refined isotropically. Other hydrogens were calculated by geometrical methods and refined using a riding model. Crystallographic data have been deposited at the CCDC, 12 Union Road, Cambridge CB2 1EZ, UK and copies can be obtained on request, free of charge, by quoting the publication citation and the deposition numbers 218546–218550.

Results

Co_5 Complex 2. Reaction of $Co(AcO)_2$ in MeOH/MeCN and H_6L in CH_2Cl_2 gave pink crystals of $[Co_5(L)(\mu_4$-OH)(μ-AcO)(μ-OMe)($MeOH)_4$]AcO (**2**). The structure of the cation is shown in Fig. 1 and selected bond distances and angles are summarized in Table 2. The complex possesses a crystallographic mirror plane including Co3, S1, and S4. L^{6-} in **2** takes a pinched-cone conformation having a pocket-like structure where four phenoxo oxygens (O1, O3, O1*, and O3*) are arranged in a square planar manner. The apex cobalt(II) (Co3) is located slightly below the O_4 plane (0.670(2) Å; Co3–O = 2.063(3) and 2.075(3) Å) and is additionally coordinated by two sulfur atoms (S1 and S4, 2.5664(18) and 2.5276(19) Å, respectively), meaning Co3 has a distorted trigo-

Table 1. Crystallographic Data and Experimental Details for **2**·CH_3CN, **3**·$4H_2O$·$9CHCl_3$, **4**·$2.5CH_3CN$·$6.5CH_3OH$, **5**·$8.5H_2O$·$CHCl_3$·CH_3CN·$0.5C_2H_5OH$, and **6**·$6.5H_2O$·DMF

Complex	**2**·CH_3CN	**3**·$4H_2O$·$9CHCl_3$	**4**·$2.5CH_3CN$·$6.5CH_3OH$	**5**·$8.5H_2O$·$CHCl_3$·CH_3CN ·$0.5C_2H_5OH$	**6**·$6.5H_2O$·DMF
Empirical formula	$C_{71}H_{92}Co_5NO_{16}S_6$	$C_{86}H_{112}Ni_4Cl_{27}N_3O_{21}S_6$	$C_{79.5}H_{119.5}CoN_{2.5}Ni_4O_{22.5}S_6$	$C_{72}H_{113}Cl_3MnNNi_4O_{25}S_6$	$C_{69}H_{86}CuNNi_4O_{23.5}S_6$
Formula weight	1702.47	2911.01	1956.41	1981.12	1795.62
Temperature/K	183(2)	213(2)	293(2)	293(2)	180(2)
Crystal system	Monoclinic	Monoclinic	Triclinic	Triclinic	Hexagonal
Space group	$C2/m$	$C2/c$	$P\bar{1}$	$P\bar{1}$	$P6_3/m$
a/Å	19.706(4)	32.586(3)	17.694(2)	17.7333(14)	30.9481(15)
b/Å	22.822(4)	14.3252(12)	18.135(2)	18.1757(15)	30.9481(15)
c/Å	19.254(4)	28.610(2)	19.271(2)	19.3619(16)	17.0920(13)
α/°			89.615(3)	90.187(3)	
β/°	113.296(5)	100.749(3)	73.886(3)	105.753(3)	
γ/°			62.061(3)	118.037(3)	
V/Å^3	7953(2)	13120.7(19)	5192.7(11)	5238.1(7)	14177.2(15)
Z	4	4	2	2	6
μ(Mo Kα)/mm^{-1}	1.24	1.275	1.05	1.079	1.197
Crystal size/mm^3	0.55 × 0.40 × 0.10	0.50 × 0.30 × 0.15	0.85 × 0.10 × 0.10	0.70 × 0.10 × 0.10	0.40 × 0.15 × 0.10
Reflections collected	23975	41456	43984	36834	88963
Independent reflections (R(int))	7198 (0.0901)	12677 (0.0543)	19914 (0.0945)	13684 (0.1110)	8618 (0.1194)
Max. and min. transmission	0.8860 and 0.5487	0.8326 and 0.5698	0.9023 and 0.4690	0.8998 and 0.5189	0.8897 and 0.6460
Data/restraints/parameters	7198/0/558	12677/0/861	19914/0/1200	13684/0/1254	8618/0/568
Goodness-of-fit on F^2	0.991	0.951	0.842	0.811	0.914
R indices ($I > 2\sigma(I)$)[a)]	$R1 = 0.059$, $wR2 = 0.144$	$R1 = 0.064$, $wR2 = 0.153$	$R1 = 0.062$, $wR2 = 0.137$	$R1 = 0.067$, $wR2 = 0.177$	$R1 = 0.076$, $wR2 = 0.188$
R indices (all data)[a)]	$R1 = 0.093$, $wR2 = 0.169$	$R1 = 0.114$, $wR2 = 0.173$	$R1 = 0.170$, $wR2 = 0.166$	$R1 = 0.187$, $wR2 = 0.211$	$R1 = 0.155$, $wR2 = 0.226$
Largest diff. peak and hole/e Å^{-3}	1.354 and −1.166	0.839 and −0.433	0.707 and −0.399	0.722 and −0.481	1.136 and −0.444

a) $R1 = \Sigma\|F_o| - |F_c\|/\Sigma|F_o|$, $wR2 = [\Sigma w(F_o^2 - F_c^2)^2/\Sigma w(F_o^2)^2]^{1/2}$.

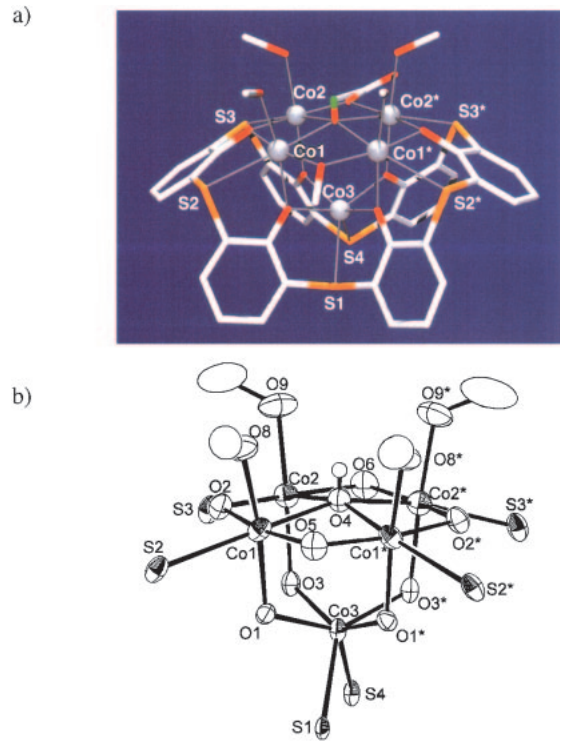

Fig. 1. a) Crystal structure of the cation of **2**. *tert*-Butyl groups are omitted. b) ORTEP diagram of pentacobalt(II) core with thermal ellipsoids at 40% probability. Asterisked atoms were generated using the symmetry transformation $x, -y, z$.

Table 2. Selected Bond Distances (Å) and Angles (°) for **2**

Co1–O1	2.070(3)	Co1–O2	2.009(3)
Co1–O4	2.270(3)	Co1–O5	1.995(3)
Co1–O8	2.091(4)	Co1–S2	2.5817(15)
Co2–O2	1.991(3)	Co2–O3	2.054(3)
Co2–O4	2.219(4)	Co2–O6	2.057(3)
Co2–O9	2.092(4)	Co2–S3	2.5155(15)
Co3–O1	2.063(3)	Co3–O3	2.075(3)
Co3–S1	2.5664(18)	Co3–S4	2.5276(19)
Co1–O4–Co1*	86.26(17)	Co1–O5–Co*	102.1(2)
Co1–O2–Co2	103.01(15)	Co1–O4–Co2	88.44(6)
Co1–O4–Co2*	160.2(3)	Co1–O1–Co3	114.44(14)
Co2–O4–Co1*	160.2(3)	Co2–O4–Co2*	90.16(18)
Co2–O6–Co2*	99.6(2)	Co2–O3–Co3	117.35(15)

Asterisked atoms were generated using the symmetry transformation $x, -y, z$.

nal prism geometry with the two trigonal planes defined by O1/O1*/S1 and O3/O3*/S4. The basal cobalt(II) ions (Co1, Co2, Co1*, and Co2*) are located above the phenoxo oxygens and are in a similar octahedral coordination. Each cobalt(II) is coordinated by two phenoxo oxygens (2.070(3) and 2.054(3) Å for O1 and O3; 2.009(3) and 1.991(3) Å for O2), a sulfur (2.5817(15) and 2.5155(15) Å), a μ_4-hydroxo (O4, 2.270(3) and 2.219(4) Å), a μ_2-methoxo or a μ_2-acetate (O5 or O6, 1.995(3) and 2.057(3) Å), and a methanol oxygen (O8 and O9, 2.091(4) and 2.092(4) Å). A counter acetate forms a hydrogen bond with the μ_4-hydroxo group ($O4\cdots O_{acetate} = 3.020(9)$ Å), of which the hydrogen atom was found by differential Fourier synthesis.

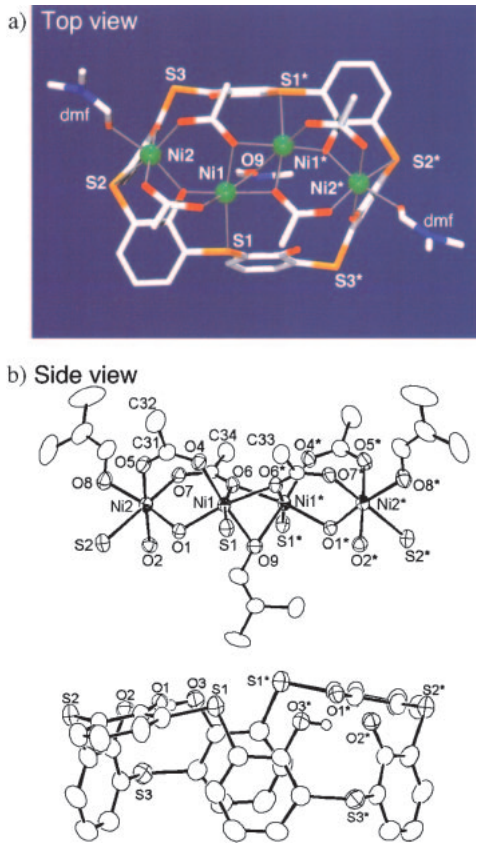

Fig. 2. a) Top view of the crystal structure of the Ni^{II}_4 complex **3**. b) Side view of the ORTEP diagrams of the Ni_4 core[17] and the H_2L^{4-} with thermal ellipsoids at 40% probability. The *tert*-butyl groups and the hydrogens, except for the phenolic hydrogens, are omitted. Asterisked atoms were generated using the symmetry transformation $-x + 1, y, -z + 3/2$.

Table 3. Selected Bond Distances (Å) and Angles (°) for **3**

Ni1–O1	1.9911(12)	Ni1–O4	2.0041(13)
Ni1–O6	2.0418(11)	Ni1–O6*	2.0648(12)
Ni1–O9	2.1699(13)	Ni1–S1	2.4309(5)
Ni1–Ni1*	2.9186(5)	Ni2–O1	2.1014(11)
Ni2–O2	2.0252(12)	Ni2–O5	2.0408(12)
Ni2–O7	2.0274(12)	Ni2–O8	2.0834(12)
Ni2–S2	2.4271(6)		
Ni1–O1–Ni2	108.71(5)	Ni1–O6–Ni1*	90.58(4)
Ni1*–O9–Ni1	84.52(6)		

Asterisked atoms were generated using the symmetry transformation $-x + 1, y, -z + 3/2$.

Ni_4 Complex 3. Reaction of $Ni(AcO)_2$ in MeOH and H_6L in $CHCl_3$ gave a green complex (in 67% yield) having a completely different structure from **1** and **2**. The structure of the resulting tetranickel(II) complex, $[Ni_4(H_2L)(AcO)_4(\mu\text{-dmf})(dmf)_2]$ (**3**), is shown in Fig. 2,[17] and selected bond distances and angles are summarized in Table 3. The complex possesses

a crystallographic two-fold axis passing through the midpoint of Ni1–Ni1*, and hence the half of the complex is crystallographically independent. In **3**, diprotonated H_2L^{4-} takes a cone conformation with the donor atom set in a planar arrangement (O1, O2, S1, S2, and their asterisked atoms related by a two-fold axis, Fig. 2(b)), and contains four nickel(II) ions arranged in a zigzag chain on the donor plane. The H_2L^{4-} binds Ni1 via a phenoxo oxygen (O1) and a sulfur (S1, 2.4309(5) Å) and Ni2 via two phenoxo oxygens (O1 and O2) and a sulfur (S2, 2.4271(6) Å). The nickel(II) ions are additionally bridged by two acetate ions (Ni1···Ni2) or two acetate ions and a dmf oxygen (Ni1···Ni1*). One acetate bridges three nickel ions via O7 in μ_1-manner and O6 in μ_2-manner. A dmf molecule is encapsulated in the cavity of conic H_2L^{4-} which bridges Ni1 and Ni1* via O9. Two sulfur (S3 and S3*) and two phenol oxygen atoms (O3 and O3*) of H_2L^{4-} are not coordinate. A phenol proton was found near O3 by differential Fourier synthesis, which means that O3 and O2 are connected by a hydrogen bond.

Solution Studies by MS Spectrometry. Since the tetranickel(II) **3** has four coordination free donor atoms (S3, S3*, O3 and O3*), the complex itself can act as a ligand. To determine if **3** can act as a "metal-including ligand", reactions of **3** with other metal ions were investigated using ESI mass spectrometry.

Figure 3(a) shows the ESI mass spectrum of **3** using a $CHCl_3$/EtOH solvent mixture. A peak centered around $m/z =$ 1751.1 corresponding to $\{Ni_4(H_2L)(AcO)_3(dmf)_2(CHCl_3)\}^+$, or $\{\mathbf{3} - AcO^- - dmf + CHCl_3\}^+$, was observed. The presence of $CHCl_3$ was confirmed by comparison with the isotope pattern. The result shows that the tetranickel(II) core structure remains intact in solution.

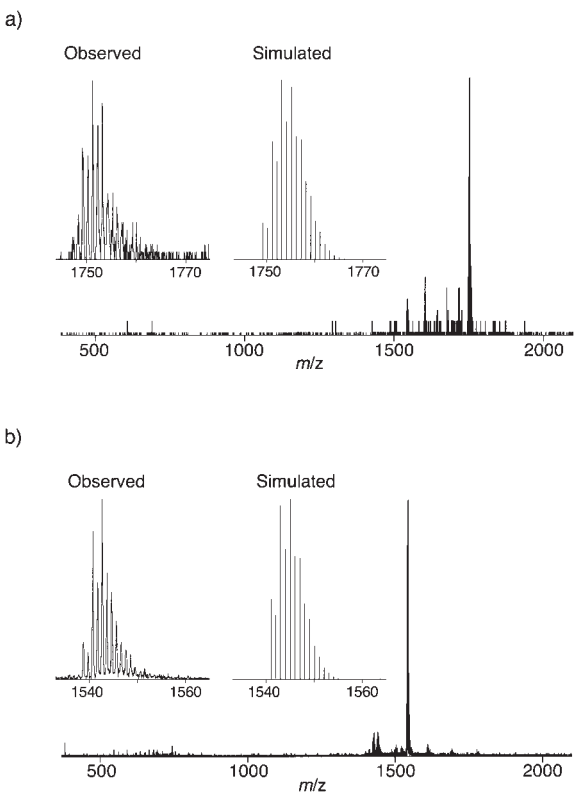

Fig. 3. ESI Mass-spectra of (a) complex **3** and (b) a mixture of manganese(II) acetate and **3** in a 1:1 ratio.

One equivalent of $Mn(AcO)_2$ in MeOH was added to a solution of **3** in $CHCl_3$ at room temperature; next the solvent was evaporated and the residue was dissolved in $CHCl_3$/EtOH mixed solution. The tetranickel(II) species nearly disappeared (Fig. 3(b)) and a new sharp signal appeared, centered around $m/z = 1542.8$. Reactions with $Co(AcO)_2$ or $Cu(AcO)_2$ in a 1:1 molar ratio also showed similar spectral changes, giving a new peak centered around $m/z = 1546.6$ for cobalt(II) and 1549.6 for copper(II), respectively. The differences in m/z values for the new compounds correspond to the differences in atomic weights among manganese, cobalt, and copper atoms. Therefore the new signals were assigned to be the mixed metal pentanuclear complex, $\{MNi_4(L)(OH)(AcO)_2(EtOH)\}^+$, an analog of **2** ($\{Co_5(L)(\mu_4\text{-OH})(\mu\text{-AcO})(\mu\text{-OMe})(MeOH)_4\}^+$). These spectral changes clearly indicate that **3** can act as a "metal-involving ligand" for manganese(II), cobalt(II), and copper(II) ions. Crystals of these complexes were obtained from the appropriate reaction solution, and the assignments for the signals were proven to be correct using X-ray crystallography.

Reaction of nickel(II) acetate and **3** in a 1:1 molar ratio gave a similar change in the mass spectrum, but crystals could not be obtained from the reaction solution. An insoluble precipitate formed which may be due to a polymerization reaction involving the pentanickel complex. A discrete pentanickel complex would be unstable and easily polymerize under this condition.

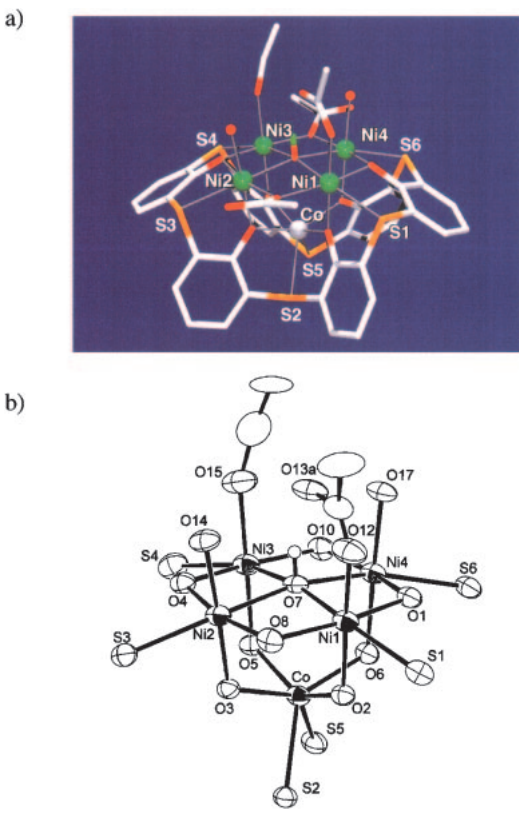

Fig. 4. a) Crystal structure of the monocobalt(II)tetranickel(II) complex **4**.[17] *tert*-Butyl groups are omitted. b) ORTEP diagram of monocobalt(II)tetranickel(II) core with thermal ellipsoids at 40% probability.

Table 4. Selected Bond Distances (Å) and Angles (°) for **4**, **5**, and **6**

	4	**5**		**6**
	M = Co	M = Mn		
M–O2	2.0739(15)	2.1072(17)	Cu–O2	1.973(4)
M–O3	2.0683(10)	2.123(3)	Cu–O3	1.990(5)
M–O5	2.0684(14)	2.117(2)		
M–O6	2.0620(12)	2.108(2)		
M–S2	2.5840(6)	2.7184(11)	Cu–S2	2.857(2)
M–S5	2.5887(6)	2.7276(10)		
Ni1–O1	1.9789(11)	1.968(2)	Ni1–O1	1.977(4)
Ni1–O2	2.0353(13)	2.024(2)	Ni1–O2	2.048(4)
Ni1–O7	2.1844(14)	2.231(2)	Ni1–O5	2.229(5)
Ni1–O8	2.0622(12)	2.009(3)	Ni1–O6	2.040(6)
Ni1–O12	2.0411(16)	2.065(2)	Ni1–O8	2.030(6)
Ni1–S1	2.4883(7)	2.4833(12)	Ni1–S1	2.490(2)
Ni2–O3	2.0225(12)	2.021(2)	Ni2–O3	2.046(5)
Ni2–O4	1.9851(14)	1.9640(19)	Ni2–O4	1.994(5)
Ni2–O7	2.2376(12)	2.179(3)	Ni2–O5	2.218(5)
Ni2–O8	2.0251(15)	2.057(2)	Ni2–O6	2.045(6)
Ni2–O14	2.0719(13)	2.062(3)	Ni2–O11	2.067(6)
Ni2–S3	2.4863(7)	2.4809(12)	Ni2–S3	2.477(3)
Ni3–O4	1.9650(11)	1.992(3)		
Ni3–O5	2.0302(13)	2.031(2)		
Ni3–O7	2.2155(15)	2.277(2)		
Ni3–O10	2.0512(12)	2.032(3)		
Ni3–O13	2.0555(15)	2.080(2)		
Ni3–S4	2.4874(8)	2.4884(10)		
Ni4–O1	1.9854(15)	1.9814(19)		
Ni4–O6	2.0357(13)	2.025(2)		
Ni4–O7	2.2287(11)	2.239(3)		
Ni4–O10	2.0427(15)	2.060(2)		
Ni4–O16	2.0754(14)	2.025(3)		
Ni4–S6	2.4826(6)	2.4912(15)		
Ni1–O2–M	115.82(6)	114.29(11)	Cu–O2–Ni1	109.3(2)
Ni2–O3–M	116.01(6)	113.94(10)	Cu–O3–Ni2	109.4(2)
Ni3–O5–M	115.62(7)	113.57(7)		
Ni4–O6–M	115.36(4)	113.72(12)		
Ni1–O7–Ni2	90.16(4)	90.94(8)	Ni1–O5–Ni2	89.58(6)
Ni1–O8–Ni2	100.02(5)	101.30(9)	Ni1–O6–Ni2	100.1(2)
Ni1–O7–Ni3	167.68(6)	169.32(11)	Ni1–O5–Ni2*	164.1(3)
Ni1–O1–Ni4	102.47(7)	105.73(12)	Ni1–O1–Ni1*	104.0(3)
Ni1–O7–Ni4	88.91(5)	89.53(10)	Ni1–O5–Ni1*	88.7(2)
Ni2–O4–Ni3	103.66(7)	104.07(12)	Ni2–O4–Ni2*	100.9(3)
Ni2–O7–Ni3	88.43(5)	88.83(9)	Ni2–O5–Ni2*	87.8(2)
Ni2–O7–Ni4	166.02(6)	170.68(10)		
Ni3–O7–Ni4	89.50(4)	88.99(7)		
Ni3–O10–Ni4	99.68(5)	101.33(9)		

Asterisked atoms were generated using the symmetry transformation x, y, $-z + 1/2$.

Mixed Metal MNi_4 Complexes. As shown from the solution studies, the reaction of tetranickel(II) complex and cobalt(II) acetate in a 1:1 reaction ratio on a synthetic scale gave the mixed-metal pentanuclear cluster complex $[CoNi_4(L)(\mu_4\text{-}OH)(\mu\text{-}AcO)_2(AcO)(H_2O)_2(EtOH)]$ (**4**)[17] in an almost quantitative yield (~90%). The structure of **4**, Fig. 4, involves the pentanuclear moiety, $\{CoNi_4(L)(\mu_4\text{-}OH)(\mu\text{-}AcO)_2(EtOH)\}^+$, observed in the mass spectrometry. Selected atom–atom distances and angles for **4** are summarized in Table 4 along with the data for other mixed-metal complexes.

The structure of **4** is similar to **2** with L^{6-} taking a pinched-cone conformation. There are five metal ions in the pocket of pinched-conic L^{6-} in a pyramidal arrangement. The apex metal ion (M_{apex}) is surrounded by four phenoxo oxygen atoms and two sulfur atoms from L^{6-} in a distorted trigonal prismatic manner with two basal planes defined by SO_2 donor sets. The coordination distances are 2.0620(12)–2.0739(15) Å for phenoxo oxygens and 2.5840(6) and 2.5887(6) Å for sulfurs, respectively. As M_{apex} is in completely the same coordination environment as that observed for Co3 in **2**, M_{apex} is assigned to

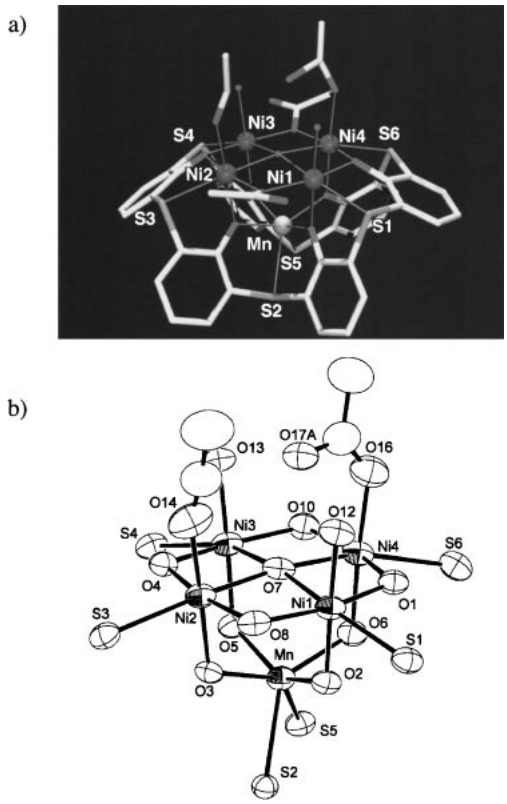

Fig. 5. a) Crystal structure of the monomanganese(II)tetranickel(II) complex **5**.[17] *tert*-Butyl groups are omitted. b) ORTEP diagram of monomanganese(II)tetranickel(II) core with thermal ellipsoids at 40% probability.

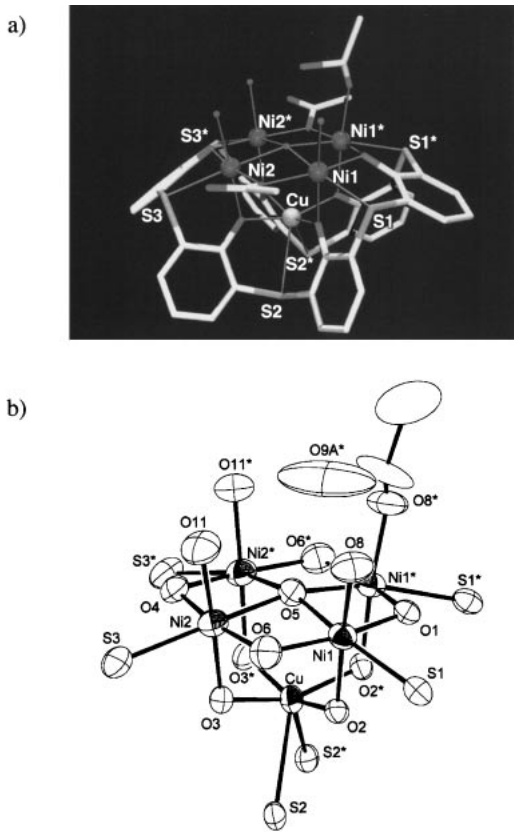

Fig. 6. a) Crystal structure of the monocopper(II)tetranickel(II) complex **6**.[17] *tert*-Butyl groups are omitted. b) ORTEP diagram of monocopper(II)tetranickel(II) core with thermal ellipsoids at 40% probability. Asterisked atoms were generated using the symmetry transformation x, y, $-z + 1/2$.

be a cobalt(II) ion. The basal nickel(II) ions are in an octahedral coordination; each basal nickel(II) ion is bound to O_2S donor set from L^{6-} having shorter Ni–S distances (Ni–S = 2.4826(6)–2.4883(7) Å) than the basal Co–S in **2**. The cobalt(II) and nickel(II) ions are bridged by phenoxo oxygens in the bond range between 2.0225(12)–2.0357(13) Å. Two other phenoxo oxygens from L^{6-} (O1 and O4) bridge the nickel(II) ions with the shorter distances of 1.9650(11)–1.9854(15) Å. The nickel(II) ions are further bridged by a μ_4-hydroxo group (O7 with the distances of 2.1844(14)–2.2376(12) Å) and μ_2-acetate-κ^2O groups (O8 and O10, 2.0251(15)–2.0622(12) Å), and each octahedron is completed by an acetate (Ni1), a water (Ni2 and Ni4), or an EtOH (Ni3).[18]

Reaction of **3** and manganese(II) acetate or copper(II) acetate resulted in a similar core rearrangement giving $[MnNi_4(L)(\mu_4\text{-}OH)(\mu\text{-}AcO)_2(AcO)(H_2O)_2(EtOH)]$ (**5**) and $[CuNi_4(L)(\mu_4\text{-}OH)(\mu\text{-}AcO)_2(AcO)(H_2O)_3]$ (**6**). The structures of these complexes are shown in Figs. 5 and 6. **6** possesses a crystallographic mirror plane including O1, Cu, and O4, and half of the molecule is independent. The terminal acetate group including O8 is disordered with the two positions related to the mirror plane; one possibility is depicted in Fig. 6. The structures of $MnNi_4$ and $CuNi_4$ are similar to **4**, with the apex position occupied by M^{II} ion and the basal positions by Ni^{II} ions. In these complexes, the apex M ions are in a distorted trigonal prismatic coordination environment with trigonal planes defined by O2/O3/S2 and O5/O6/S5 for **5** and O2/O3/S2 for **6**, having typical bond lengths depending on the metal ions. The distances around Mn are longer in the $MnNi_4$ complex (Mn–S = 2.7184(11) and 2.7276(10) Å, and Mn–O = 2.1072(17)–2.123(3) Å) than in other complexes. The Cu in the $CuNi_4$ complex is also in a distorted trigonal prism by O_4S_2 donor set (Cu–S = 2.857(2) Å and Cu–O = 1.973(4) and 1.990(5) Å) whereas the apex Cu in **1** is in a distorted square pyramid by O_4S. All basal nickel(II) ions in the two mixed-metal clusters are in the same octahedral coordination environment surrounded by a sulfur (2.477(3)–2.4912(15) Å), two phenoxo oxygens (1.9640(19)–1.994(5) Å for O1 and O4, and 2.021(2)–2.048(4) Å for O2, O3, O5, O6 (**5**), O2, and O3 (**6**)), a μ_4-hydroxo (O7 (**5**) and O5 (**6**), 2.179(3)–2.277(2) Å), and an oxygen from a bridging acetate (O8, O10 (**5**) and O6 (**6**), 2.009(3)–2.060(2) Å), having similar coordination distances found in the $CoNi_4$ complex. Octahedral coordination is completed by a supporting ligand such as an acetate (Ni4 in **5** and Ni1* in **6**), a water (Ni1 and Ni3 in **5** and Ni1, Ni2, and Ni2* in **6**), or an ethanol (Ni2 in **5**).[18]

The mixed-metal complexes all involve three acetate groups, of which two acetates bridge basal nickel(II) ions and one is axially bound to nickel(II) ion as a terminal ligand. In the latter acetate, one oxygen atom free from coordination is placed above the μ_4-hydroxo group to form a hydrogen bond.

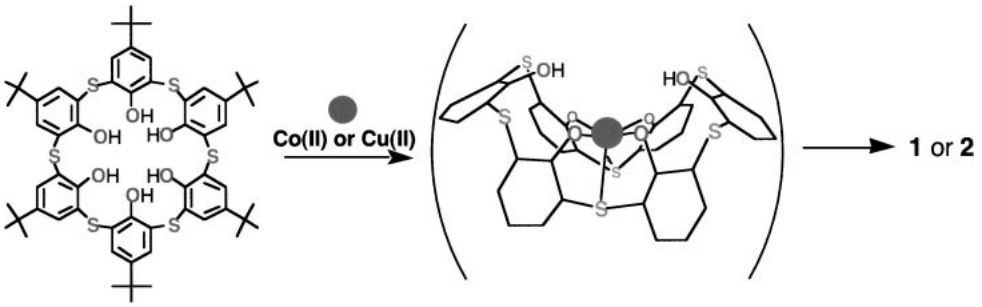

Scheme 1.

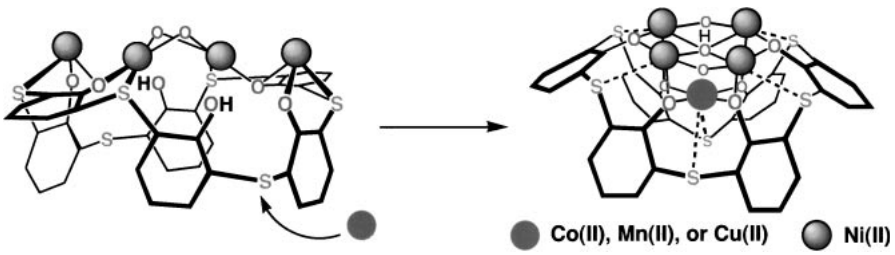

Scheme 2.

Discussion

Thiacalix[6]arene As a Clustering Ligand. We have shown that the homo-metal complex **2** and three hetero-metal complexes **4**–**6** have a similar structure, all structures are also similar to that of the decacopper(II) complex **1** that we reported previously.[12] In these complexes, five metal ions in each complex are arranged in a square-pyramidal manner and all of the metal ions are connected via phenoxo oxygens from L^{6-} and other supporting ligands such as a μ_4-hydroxo group. These results indicate the high potential of L^{6-} as a clustering ligand to give three dimensionally arranged metal cluster cores. To nickel(II) ions, the thiacalix[6]arene acts as a tetranucleating ligand to give cluster complex **3** which has a different structure than the structures of **1**, **2**, and **4**–**6**. The difference in the structures comes from the nature of the metal ions.

In the complexes except **3**, L^{6-} in a pinched-cone conformation supplies five or six donor atoms to complete the coordination geometry around the apex metal ions, i.e., O_4S donor set for copper(II) ion in highly distorted square pyramid (**1**) and O_4S_2 donor set for manganese(II), cobalt(II), and copper(II) ions in distorted trigonal prism (**2** and **4**–**6**). The chelating effect of L^{6-} for apex metal ion would be stronger than that for the basal metal ions because the latter are bound to L^{6-} via three donor atoms. Hence we assume that, at an early stage in the formation of homo-metal complexes **1** and **2**, the thiacalix[6]arene binds the first metal ion via O_4S or O_4S_2 donor set to take a pinched-cone conformation, and then other metal ions are taken up in the pocket formed (Scheme 1).[19]

On the other hand, Ni^{II} ions usually can not adopt these distorted geometries, and thus a pentanickel complex similar to **1** and **2** did not form. The calixarene takes a cone conformation in the absence of the apex metal ions, and four nickel(II) ions are placed on a donor surface of the H_2L^{4-} to give **3**. However, thiacalix[6]arene also acts as a clustering ligand to nickel(II) ions showing a different manner from that in **1**, **2**, and **4**–**6**. The conic H_2L^{4-} has a cavity and one dmf molecule is encapsulated to bridge the nickel(II) ions.

Formation of Mixed-Metal Pentanuclear Complexes via Ni_4 Core Rearrangement. Complexes **4**–**6** are synthesized by step-by-step bottom-up reactions, a procedure which is novel in the area of mixed metal arrays. The formation of the mixed-metal complexes via Ni_4 core rearrangement is induced by metal-insertions. The core rearrangement involving **3**, which occurs upon reaction with manganese(II), cobalt(II), or copper(II) ion, causes acetate ions to be released. In the resulting pentanuclear complexes, the number of bridging acetates has decreased from four to two, as was confirmed by the mass spectrometry. As mentioned above, it is thought that the insertion of a metal ion into the apex position forces the calixarene to take a pinched-cone conformation because of its strong chelating affinity to manganese(II), cobalt(II), and copper(II) ions. In this conformation, the four nickel(II) ions are no longer able to take a zigzag arrangement, and the core-rearrangement occurs to give a square-planar arrangement having a smaller bridging ligand, μ_4-hydroxo group (Scheme 2).

A similar insertion reaction is believed to occur with nickel(II) acetate. In the mass spectrum, a reduction in mass was observed, indicating loss of acetate ions upon core rearrangement, but it is uncertain if polymerization occurred. Since a large excess of nickel(II) acetate was employed to react with H_6L, the large excess of acetate ions could prevent core rearrangement, and as a result, the tetranickel(II) complex was generated in a good yield.

Conclusion

We have shown that *p-tert*-butylthiacalix[6]arene is an excellent clustering ligand. Moreover, a novel synthetic method for making mixed-metal cluster complexes based on a metal-induced Ni_4-core rearrangement within the pocket of the *p-tert*-butylthiacalix[6]arene was developed. Further studies aimed at the synthesis of mixed metal clusters with interesting func-

tionalities and physical properties is now in progress in our laboratory.

This work was supported by a Grant-in-Aid for Scientific Research (Nos. 10149102, 14340203, and 13740370) from the Ministry of Education, Culture, Sports, Science and Technology, as well as by JSPS Research for the Future Program.

References

1 a) M. Handa, T. Takemoto, L. K. Thompson, M. Mikuriya, N. Nagao, S. Ikemi, J.-W. Lim, T. Sugimori, I. Hiromitsu, and K. Kasuga, *Chem. Lett.*, **2001**, 316. b) K. K. Nanda, K. Venkatsubramanian, D. Majumdar, and K. Nag, *Inorg. Chem.*, **33**, 1581 (1994). c) M. J. Grannas, B. F. Hoskins, and R. Robson, *Inorg. Chem.*, **33**, 1071 (1994). d) M. J. Grannas, B. F. Hoskins, and R. Robson, *J. Chem. Soc., Chem. Commun.*, **1990**, 1644.

2 a) S. S. Tandon, L. K. Thompson, J. N. Bridson, and C. Benelli, *Inorg. Chem.*, **34**, 5507 (1995). b) S. S. Tandon, L. K. Thompson, and J. N. Bridson, *J. Chem. Soc., Chem. Commun.*, **1992**, 911. c) B. F. Hoskins, R. Robson, and P. Smith, *J. Chem. Soc., Chem. Commun.*, **1990**, 488. d) H. C. Aspinall, J. Black, I. Dodd, M. M. Harding, and S. J. Winkley, *J. Chem. Soc., Dalton Trans.*, **1993**, 709.

3 a) S. Brooker, V. McKee, W. B. Shepard, and L. K. Pannell, *J. Chem. Soc., Dalton Trans.*, **1987**, 2555. b) V. McKee and W. B. Shepard, *J. Chem. Soc., Chem. Commun.*, **1985**, 158.

4 a) S. Cromie, F. Launay, and V. McKee, *Chem. Commun.*, **2001**, 1918. b) M. Yonemura, H. Okawa, M. Ohba, D. E. Fenton, and L. K. Thompson, *Chem. Commun.*, **2000**, 817.

5 a) V. McKee and S. S. Tandon, *J. Chem. Soc., Dalton Trans.*, **1991**, 221. b) V. McKee and S. S. Tandon, *Inorg. Chem.*, **28**, 2901 (1989).

6 a) J. McCrea, V. McKee, T. Metcalfe, S. S. Tandon, and J. Wikaira, *Inorg. Chim. Acta*, **297**, 220 (2000). b) P. E. Kruger, F. Launay, and V. McKee, *Chem. Commun.*, **1999**, 639. c) E. Asato, H. Furutachi, T. Kawahashi, and M. Mikuriya, *J. Chem. Soc., Dalton Trans.*, **1995**, 3897. d) M. Bell, A. J. Edwards, B. F. Hoskins, E. H. Kachab, and R. Robson, *J. Am. Chem. Soc.*, **111**, 3603 (1989). e) A. J. Edwards, B. F. Hoskins, E. H. Kachab, A. Markiewicz, K. S. Murray, and R. Robson, *Inorg. Chem.*, **31**, 3585 (1992).

7 a) C. D. Gutsche, "Calixarenes Revisited, Monographs in Supramolecular Chemistry," ed by J. F. Stoddart, The Royal Society of Chemistry, Cambridge (1998). b) H. S. Park, Q. Lin, and A. D. Hamilton, *J. Am. Chem. Soc.*, **121**, 8 (1999).

8 N. Iki, N. Morohashi, C. Kabuto, and S. Miyano, *Chem. Lett.*, **1999**, 219.

9 a) H. Akdas, E. Graf, M. W. Hosseini, A. De Cian, A. Bilyk, B. W. Skelton, G. A. Koutsantonis, I. Murray, J. M. Harrowfield, and A. H. White, *Chem. Commun.*, **2002**, 1042. b) A. Bilyk, A. K. Hall, J. M. Harrowfield, M. W. Hosseini, B. W. Skelton, and A. H. White, *Inorg. Chem.*, **40**, 672 (2001). c) Z. Asfari, A. Bilyk, J. W. C. Dunlop, A. K. Hall, J. M. Harrowfield, M. W. Hosseini, B. W. Skelton, and A. H. White, *Angew. Chem., Int. Ed.*, **40**, 721 (2001). d) H. Akdas, E. Graf, M. W. Hosseini, A. de Cian, and J. M. Harrowfield, *Chem. Commun.*, **2000**, 2219.

10 N. Morohashi, N. Iki, S. Miyano, T. Kajiwara, and T. Ito, *Chem. Lett.*, **2001**, 66.

11 a) T. Kajiwara, S. Yokozawa, T. Ito, N. Iki, N. Morohashi, and S. Miyano, *Chem. Lett.*, **2001**, 6. b) T. Kajiwara, S. Yokozawa, T. Ito, N. Iki, N. Morohashi, and S. Miyano, *Angew. Chem., Int. Ed.*, **41**, 2076 (2002).

12 T. Kajiwara, N. Kon, S. Yokozawa, T. Ito, N. Iki, and S. Miyano, *J. Am. Chem. Soc.*, **124**, 11274 (2002).

13 a) N. Iki and S. Miyano, *J. Inclusion Phenom. Macrocyclic Chem.*, **41**, 99 (2001). b) N. Iki, N. Morohashi, T. Suzuki, S. Ogawa, M. Aono, C. Kabuto, H. Kumagai, H. Takeya, S. Miyanari, and S. Miyano, *Tetrahedron Lett.*, **41**, 2587 (2000). c) N. Kon, N. Iki, and S. Miyano, *Tetrahedron Lett.*, **43**, 2231 (2002). d) N. Morohashi, N. Iki, M. Aono, and S. Miyano, *Chem. Lett.*, **2002**, 494.

14 SAINT and XPREP, Area detector data integration and reduction software, Bruker Analytical X-ray Instruments Inc., Madison, WI, 1995.

15 A. Altomare, M. C. Burla, M. Camalli, M. Cascarano, C. Giacovazzo, A. Guagliardi, and G. Polidori, *J. Appl. Crystallogr.*, **27**, 435 (1994).

16 G. M. Sheldrick, University of Göttingen, Germany, 1997.

17 Disorder was found in a bridging dmf in **3**, coordinated acetate and ethanol in **4** and **5**, and coordinated acetate and water in **6**. One of two possibilities is shown in Figs. 2 and 4–6.

18 The coordinating ethanol molecules would come from chloroform which contains ethanol (∼1%) as a stabilizer. Another possibility involving acetonitrile as an axial ligand in complexes **4** and **5** is denied by the results of the elemental analysis.

19 We also succeeded to synthesize a trimanganese(II) complex in which the apex and two basal positions of the pinched-conic L^{6-} are occupied by manganese(II) ions. T. Kajiwara, R. Shinagawa, T. Ito, N. Kon, N. Iki, and S. Miyano, unpublished results.